



# Agreement between Murray law-based quantitative flow ratio ( $\mu$ QFR) and three-dimensional quantitative flow ratio (3D-QFR) in non-selected angiographic stenosis: A multicenter study

Carlos Cortés<sup>1\*</sup> , Lili Liu<sup>2\*</sup>, Scarlet Luisa Berdin<sup>3, 4</sup>, Pablo M. Fernández-Corredoira<sup>1</sup>, Ruiyan Zhang<sup>2</sup>, Ulrich Schäfer<sup>5</sup>, María López<sup>6</sup>, José A. Diarte<sup>1</sup>, Shengxian Tu<sup>7</sup>, Juan Luis Gutiérrez-Chico<sup>2, 5</sup> 

<sup>1</sup>Miguel Servet University Hospital, Zaragoza, Spain

<sup>2</sup>Department of Cardiovascular Medicine, Ruijin Hospital,

Shanghai Jiao Tong University School of Medicine, Shanghai, China

<sup>3</sup>Bundeswehrkrankenhaus (Federal Army Military Hospital), Hamburg, Germany

<sup>4</sup>Asklepios Klinik St. Georg (Asklepios St. Georg Clinic), Hamburg, Germany

<sup>5</sup>Bundeswehrzentral Krankenhaus (Federal Army Central Military Hospital), Koblenz, Germany

<sup>6</sup>Nursing High School, University of Valladolid, Valladolid, Spain

<sup>7</sup>Med-X Research Institute, School of Biomedical Engineering, Shanghai Jiao Tong University, Shanghai, China

This paper was guest edited by Prof. Tomasz Roleder

## Abstract

**Background:** *The agreement between single-projection Murray-based quantitative flow ratio ( $\mu$ QFR) and conventional three-dimensional quantitative flow ratio (3D-QFR) has not been reported hitherto.*

**Methods:** *Patients from a multinational database were randomly selected for the study of agreement, according to sample size calculation. Both conventional 3D-QFR and  $\mu$ QFR were analyzed for all available arteries at a central corelab by independent analysts, blinded to each other's results.*

**Results:** *Ninety-eight coronary arteries from 35 patients were finally analyzed. Median 3D-QFR was 0.82 (interquartile range 0.78–0.87). The intraclass correlation coefficient for the absolute agreement between 3D-QFR and  $\mu$ QFR was 0.996 (95% confidence interval [CI]: 0.993–0.997); Lin's coefficient 0.996 (95% CI: 0.993–0.997), without constant or proportional bias (intercept = 0 and slope = 1 in orthogonal regression). As dichotomous variable, there was absolute agreement between  $\mu$ QFR and 3D-QFR, resulting in no single false positive or negative. Kappa index was 1 and the diagnostic accuracy 100%.*

**Conclusions:**  *$\mu$ QFR using a single angiographic projection showed almost perfect agreement with standard 3D-QFR. These results encourage the interchangeable use of  $\mu$ QFR and 3D-QFR, which can be interesting to improve QFR feasibility in retrospective studies, wherein appropriate double angiographic projections might be challenging to obtain. (Cardiol J 2022; 29, 3: 388–395)*

**Key words:** quantitative flow ratio,  $\mu$ QFR, coronary physiology, resting index, computational physiology, Murray law, coronary heart disease

Address for correspondence: OFA Prof. Juan Luis Gutiérrez-Chico, MD, PhD, FESC, FACC, Head of Interventional Cardiology, Bundeswehrzentral Krankenhaus, Rübenerstraße 170, 56072 – Koblenz, Germany, tel: +49 26128121610, +34 615 319370, e-mail: juanluis.gutierrezchico@ictra.es

\*These authors have equally contributed.

Received: 17.04.2022

Accepted: 11.05.2022

Early publication date: 17.05.2022

This article is available in open access under Creative Commons Attribution-Non-Commercial-No Derivatives 4.0 International (CC BY-NC-ND 4.0) license, allowing to download articles and share them with others as long as they credit the authors and the publisher, but without permission to change them in any way or use them commercially.

## Introduction

Physiology-based decision-making about the need for revascularization in patients with stable coronary heart disease has consistently proven better clinical outcomes than a merely anatomical approach [1–5]. Notwithstanding this compelling evidence, the penetration of physiology in real-world surveys is still scarce [6–10], although modestly increasing over time [11]. Against current guideline recommendations [12], the indication for revascularization in most patients with chronic coronary syndromes still relies on coronary angiography alone, without a proper functional assessment [6–10]. The reasons for this evidence-reality mismatch are multifactorial: the increase in costs and in procedural complexity of wire-based physiology, patient's discomfort during the induction of hyperemia, gaps in the operator training or the inertia of interventional teams to change their traditional *modus operandi* have been advocated to explain this phenomenon [8, 9, 13, 14].

Computational physiology has been developed to overcome the limitations of wire-based physiology and to increase the penetration of invasive functional assessment in coronary stenosis. The basic concept of computational physiology consists of an imaging-based rendering of the coronary anatomy to subsequently apply computational fluid dynamics, with the aim of estimating the pressure drop along the artery [10, 15, 16]. Intense research on this topic has resulted in a substantial simplification of the process, up to the point of circumventing the computational fluid dynamics simulation and substituting it for faster algorithms that allow a remarkably accurate estimation of fractional flow reserve (FFR) in a few seconds [14, 17]. Likewise, specific computational physiology algorithms are currently available for different imaging modalities: coronary angiography [15, 17–19], optical coherence tomography [14], intravascular ultrasound [20] or even non-invasive computed tomography angiography [21].

Quantitative flow ratio (QFR) is the most widespread method of computational physiology based on coronary angiography. Although several studies have proven the outstanding accuracy of QFR to estimate FFR [15, 17–19], the requirement of two good-quality orthogonal/separate projections for the three-dimensional (3D) rendering of the coronary lumen cannot be always accomplished, thus resulting in a proportion around 15% of cases unsuitable for analysis in retrospective studies [19, 22]. Murray law-based QFR ( $\mu$ QFR) is a novel computational method that enables accurate esti-

mation of FFR based on the analysis of a single angiographic projection with adequate quality [23], adjusting both the reference vessel diameter and the outgoing flow through side branches according to fractal geometry [16, 24]. A post-hoc analysis of patients recruited in the FAVOR (Functional Diagnostic Accuracy of Quantitative Flow Ratio in Online Assessment of Coronary Stenosis) II China study (NCT03191708) has reported excellent agreement between  $\mu$ QFR and FFR [23]. Nonetheless, agreement between  $\mu$ QFR and standard QFR based on 3D lumen reconstruction has not been reported hitherto, thus leaving a gap in the evidence about whether both methods could be indistinctly applicable in retrospective studies, depending on the quality of the angiographic projections available.

## Methods

### Study population

Real-world patients from two different retrospective cohorts, with clinical suspicion of stable coronary heart disease were screened for the current study. Inclusion criteria were: 1) having undergone a coronary angiography between 2015 and 2021; 2) mild to severe stenosis in  $\geq 1$  major coronary artery. Exclusion criteria were: hemodynamic or electrical instability at the moment of angiography acquisition; the analyzed lesion being the culprit vessel of an acute coronary syndrome in the past 7 days; chronic total occlusion of any coronary artery; bypass graft connected to the target vessel; presence of a stent in the target vessel or impossibility to provide informed consent to the analysis. Patients stemmed from a multicenter national registry of stable coronary heart disease in Spain (NCT05251012, Spanish cohort) and from Ruijin University Hospital in Shanghai (Chinese cohort). In order to shorten the analysis time, a sample of 35 patients, according to sample size calculation, were randomly selected for the study, using a computer-generated sequence of random numbers between 0 and 1, that were consecutively adjudicated to the patients. The patients with the highest adjudicated random score were selected until completing the predefined sample in a 3:2 ratio between the Spanish and Chinese cohorts, respectively, as agreed upon by the investigators.

The study complied with the principles of good clinical practice and with the Declaration of Helsinki for investigations in human beings. The study protocol was approved by the corresponding Ethics Committee and institutional review boards. All patients signed

informed consent to the anonymized use of their personal data for scientific or quality-control purposes.

### Angiographic analysis

Angiographic images were recorded at  $\geq 15$  frames/s by monoplane X-rays systems (Allura Xper FD20, Philips; Artist Q Zeego, Siemens; Innova IGS520, GE). Angiographic projections with minimal overlap and foreshortening at the corresponding target lesions were selected for offline analysis by two experienced and independent operators at an official and regularly audited corelab (Cardiovascular Imaging Core Laboratory of the Shanghai Jiao Tong University School of Medicine, Shanghai, China), using computerized edge-detection quantitative coronary angiography (QCA) software (AngioPlus Core, Pulse Medical Imaging Technology, Shanghai, China). All analysts were blinded to clinical, angiographic and functional data of the patients at all steps.

### Three-dimensional quantitative flow ratio (3D-QFR)

Two angiographic projections, acquired  $> 25^\circ$  apart, were used for 3D reconstruction of the target arteries. Markers were manually placed at the proximal and distal segments of the target vessel to guide the automatic lumen contour detection. In case of misleading vessel track, additional points markers could be placed along the lumen or the vessel contour could be manually edited. QCA was performed, reporting reference vessel diameters, minimal lumen diameter, minimal lumen area and percent diameter/area stenosis. 3D-QFR was obtained by means of artificial-intelligence (AI)-aided computation software (AngioPlus Core, Pulse Medical Imaging Technology, Shanghai, China), combining the 3D reconstruction of the angiogram with the estimation of coronary flow rendered by AI-analysis of the coronary filling velocity, as previously described [25].

In cases where 3D-QFR could not be obtained due to recording of a single projection of the target vessel, insufficient separation of the second projection, incomplete filming of the target artery, panning or irregular coronary filling, the case was labelled as non-analysable and the causes for it were registered.

### Murray-law based quantitate flow ratio ( $\mu$ QFR)

Murray-law based quantitate flow ratio was calculated using AI-aided computation software (AngioPlus Core Pulse Medical Imaging Technol-

ogy, Shanghai, China), as previously described [23]. Briefly, a single angiographic projection, in which the coronary stenosis was best visualized, minimising foreshortening and vessel overlap, was selected by the operator. The angiographic projection could be part of the pair normally used for 3D-QFR or being a totally different projection, at the operator's discretion. The lumen contour of the main vessel and its side branches with  $> 1$  mm caliber was automatically delineated by artificial intelligence throughout the angiographic loop. The frame in which the lumen contour of the lesion was best depicted was selected by the operator for the computation.  $\mu$ QFR was then calculated, based on this single angiographic projection, but taking into account the outgoing flow through the side branches to calculate both the reference diameters and the pressure drop along the stenotic segment, according to Murray's fractal law [10, 16, 24].

A paradigmatic example of analysis by 3D-QFR and  $\mu$ QFR is presented at Figure 1.

### Statistical analysis

Dichotomous and categorical variables were presented as counts (percentages). Continuous variables were presented as mean  $\pm$  95% confidence interval (CI). 3D-QFR and  $\mu$ QFR were dichotomised with a cut-off value of 0.80, thus defining  $\leq 0.80$  as significant and  $> 0.80$  as non-significant. Continuous variables were compared with the t-Student test for unpaired samples, whilst dichotomous and categorical values were compared with the Fisher exact test. A Gaussian distribution of continuous variables was checked by means of the Saphiro-Wilk test.

Due to the difficulty of defining a gold standard for the comparison QFR vs.  $\mu$ QFR, non-parametric Passing-Bablok orthogonal regression was performed to analyze correlation and eventual bias. Constant and proportional bias were evaluated as the deviation of the intercept from 0 and the deviation of the slope from 1 in the orthogonal regression model, respectively. The agreement as continuous variables was analyzed by means of Lin's coefficient, intraclass correlation coefficients for the absolute agreement (ICCa) and the Bland-Altman method. The agreement as dichotomous variables was assessed by means of kappa coefficient.

Pre-specified subgroup analysis was performed at the Spanish and Chinese cohorts, to assess the consistency between these populations.

For sample size calculation, the diagnostic accuracy of  $\mu$ QFR to predict the significance of 3D-QFR as dichotomous variable was assumed

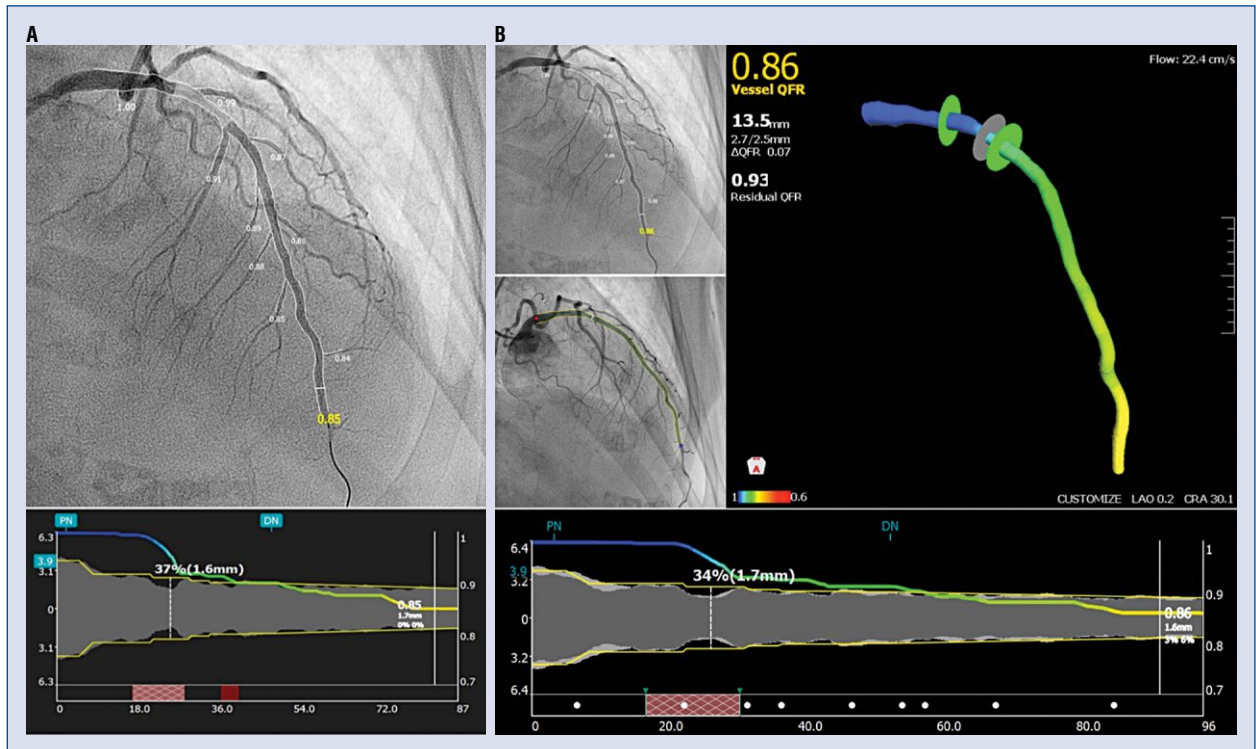


**Figure 1.** Paradigmatic example of both quantitative flow ratio (QFR) modalities:  $\mu$ QFR (A) and three-dimensional quantitative flow ratio (3D-QFR) (B).

to be superior to the agreement of the most accurate computational method to date, i.e., optical flow ratio, with a diagnostic accuracy 93% in the pivotal prospective study [14]. Therefore, assuming a diagnostic accuracy  $\geq 94\%$ , with a precision of the estimation ( $\epsilon$ ) of 5% in the interval and a 5% likelihood of  $\alpha$ -error, in two-sided calculation, the number of vessels required for a head-to-head comparison would be 87. Considering that 2.5 vessels would be on average analysable per patient, according to previous QFR multivessel studies [26], a sample of 35 patients would be able to provide sufficient statistical power to guarantee the precision of the estimation.

All statistical analysis was performed with Stata (16.1, StataCorp LLC, College Station, TX).

## Results

Between 2015 and 2021, 803 patients were included into the Spanish registry, whilst 498 coronary angiographies fulfilling the inclusion criteria were performed at the Ruijin Hospital in March 2021. After screening at the corelab, 102 patients from the Spanish cohort and 107 patients from the Chinese cohort were excluded (Fig. 2), resulting

in a total of 1092 potentially eligible patients (2878 coronary arteries), among whom 35 of them were randomly selected for the current analysis.

A total of 98 coronary arteries from 35 patients were finally analyzed: 56 (57.1%) from the Spanish cohort and 42 (42.9%) from the Chinese cohort. Patients' procedural and lesion characteristics, including QCA and computational physiology parameters of 3D-QFR and  $\mu$ QFR, are presented in Table 1. The Chinese cohort had significantly shorter lesions (17.05 vs. 24.30 mm,  $p = 0.025$ ), with a milder degree of stenosis (31.07% vs. 41.06%,  $p = 0.008$ ) than the Spanish cohort, thus resulting in a non-significant trend to higher physiology values (3D-QFR: 0.85 vs. 0.80,  $p = 0.250$ ;  $\mu$ QFR: 0.85 vs. 0.79,  $p = 0.204$ ). The three coronary territories were equally represented (left anterior descending artery: 34.69%, circumflex artery: 33.67%, right coronary artery: 31.63%).

## Agreement between 3D-QFR and $\mu$ QFR in the global sample

As continuous variables,  $\mu$ -QFR and 3D-QFR showed excellent agreement: ICCa 0.996 (95% CI: 0.993–0.997); Lin's coefficient 0.996 (95% CI: 0.993–0.997), without constant or proportional

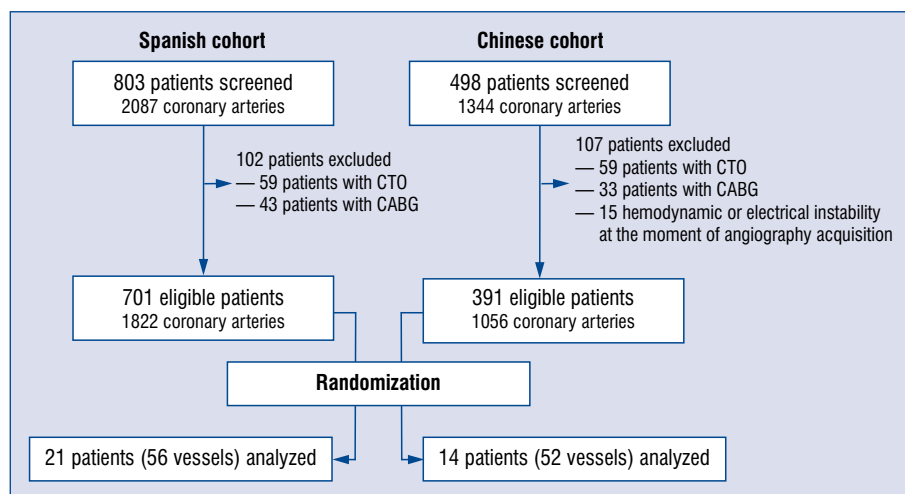


**Figure 2.** Flow chart; CABG — coronary artery bypass grafting; CTO — chronic total occlusion.

bias (intercept = 0 and slope = 1 in orthogonal regression). The estimation of the orthogonal regression line (Passing and Bablok method) and Bland-Altman graphics are represented in Figure 3.

As dichotomous variable, there was absolute agreement between  $\mu$ QFR and 3D-QFR, resulting in no single false positive or negative. Kappa index was 1 and the diagnostic accuracy 100%, meeting the premise used for sample size calculation ( $\geq 94\%$ ).

### Consistency between cohorts

Evaluating each cohort separately, the agreement between both methods showed similar values: ICCa was 0.996 (95% CI: 0.992–0.997) and 0.999 (95% CI: 0.999–0.999) in the Spanish and Chinese cohorts, respectively.

### Non-analysable cases by 3D-QFR

All cases in the study could be analyzed by  $\mu$ -QFR (retrospective feasibility 100%), whilst only 86 coronary arteries were analysable by 3D-QFR (retrospective feasibility of 87.76%). Four (4.08%) cases were unsuitable for 3D-QFR analysis due to lack of adequate second angiographic views of the target vessel for 3D reconstruction and 8 (8.16%) cases due to poor image quality with excessive overlap. The unsuitability for retrospective 3D-QFR analysis tended to be more frequent in the Spanish than in the Chinese cohort (16.1 vs. 7.1%,  $p = 0.225$ ).

## Discussion

The main findings of this study can be summarised as follows: 1) Murray-law based  $\mu$ QFR

using a single angiographic projection and standard 3D-QFR using two angiographic projections show practically perfect agreement, both as continuous or as dichotomous variables, with negligible incidence of discordant cases; 2) The retrospective feasibility of standard 3D-QFR is 87.76%, lower than reported in prospective studies, mostly due to the lack of an appropriate second projection, but it can be substantially increased in the case of  $\mu$ QFR, because it only requires a single projection of good quality per target vessel; 3) These results are consistent throughout different cohorts, stemming from different geographic regions or acquired at different times.

These results are consistent with the diagnostic accuracy reported for both methods against FFR in the FAVOR II China cohort (92.7% for 3D-QFR and 93.0% for  $\mu$ QFR) [23]. The superior agreement between both computational methods, as compared to the agreement reported for an invasive gold standard, might be considered as a proof of concept, i.e., that the simplified method, based on a single angiographic projection, preserves the rationale and the accuracy of the original 3D-QFR, whilst sparing extra time and efforts to the operator. Actually, the agreement tends to be close to perfect, with indexes close to 1 and negligible incidence of discordance in the dichotomous classification as significant/non-significant, thus confirming its huge potential for routine clinical applications.

The almost perfect agreement between both methods encourages the interchangeable use of 3D-QFR or  $\mu$ QFR in retrospective studies of computational physiology, whenever a proper 3D reconstruction of the angiography cannot be reli-

**Table 1.** Descriptive statistics of patients, intervention and lesions.

Patient level	N = 35	Spanish cohort (n = 21)	Chinese cohort (n = 14)	P
Male	25 (71.4%)	14 (66.7%)	11 (78.6%)	0.445
Age [years] (95% CI)	65.8 (61.9–72.9)	65.1 (59.6–70.6)	66.9 (61.0–72.9)	0.639
BMI (95% CI)	25.4 (24.2–26.7)	26.6 (25.0–28.2)	23.7 (22.1–25.4)	0.016
<b>Cardiovascular risk factors:</b>				
Hypertension	28 (80.0%)	18 (85.7%)	10 (71.4%)	0.301
Hypercholesterolemia	16 (45.7%)	16 (76.2%)	8 (57.1%)	0.505
Diabetes mellitus:	10 (28.6%)	8 (38.1%)	2 (14.3%)	0.127
Type 2 on OAD	8 (22.9%)	6 (28.6%)	2 (14.3%)	0.324
Type 2 on insulin	2 (5.7%)	2 (9.5%)	0 (0.0%)	0.234
Smoking:	20 (57.1%)	12 (57.1%)	8 (57.1%)	1.000
Previous smoker	8 (22.9%)	5 (23.8%)	3 (21.4%)	0.869
Current smoker	12 (34.3%)	7 (33.3%)	5 (35.7%)	0.884
Previous MI	7 (20.0%)	5 (23.8%)	2 (14.3%)	0.490
Previous revascularization	7 (20.0%)	4 (19.1%)	3 (21.4%)	0.863
GFR [mL/min] (95% CI)	77.4 (68.5–86.2)	75.1 (60.8–89.4)	80.8 (72.3–89.3)	0.530
Hemoglobin [g/dL] (95% CI)	14.0 (13.5–14.5)	14.3 (13.5–15.0)	13.5 (12.8–14.2)	0.141
LVEF [%] (95% CI)	58.8 (55.2–62.4)	54.7 (49.6–59.8)	64.9 (62.4–67.5)	0.002
<b>Procedural variables</b>				
Syntax score (95% CI)	9.3 (6.9–11.6)	9.3 (6.2–12.4)	9.2 (5.1–13.4)	0.973
Fluoroscopy [min] (95% CI)	12.2 (9.0–15.4)	12.8 (8.7–16.9)	11.3 (5.5–17.1)	0.645
<b>Clinical indication</b>				
Stable disease	29 (82.9%)	21 (100.0%)	8 (57.1%)	0.004
Unstable angina	5 (14.7%)	0 (0.0%)	5 (35.7%)	
Non-ST-elevation MI	1 (2.9%)	0 (0.0%)	1 (7.1%)	
<b>Vessels</b>				
	<b>N = 98</b>	<b>N = 56</b>	<b>N = 42</b>	0.947
LAD	34 (34.7%)	20 (35.7%)	14 (33.3%)	
LCX	33 (33.7%)	19 (33.9%)	14 (33.3%)	
RCA	31 (31.6%)	17 (30.4%)	14 (33.3%)	
Lesions (3D-QFR $\leq$ 0.80)	24 (24.5%)	18 (32.1%)	6 (14.3%)	0.057
<b>Calcification:</b>				
None to little	78 (79.6%)	42 (75.0%)	36 (87.7%)	0.216
Moderate to severe	20 (20.4%)	14 (25.0%)	6 (14.3%)	0.216
Lesion length [mm]	20.99 (18.0–24.0)	24.30 (19.5–29.1)	17.05 (13.1–21.0)	0.025
RVD [mm]	2.60 (2.5–2.7)	2.56 (2.4–2.8)	2.70 (2.5–2.9)	0.337
MLD [mm]	1.62 (1.5–1.8)	1.5 (1.3–1.6)	1.8 (1.6–2.1)	0.018
DS [%]	38.37 (34.8–42.0)	41.06 (36.9–45.2)	31.07 (24.7–37.4)	0.008
<b>3D-QFR (95% CI)</b>	<b>0.82 (0.78–0.87)</b>	<b>0.80 (0.74–0.86)</b>	<b>0.85 (0.77–0.94)</b>	<b>0.250</b>
<b><math>\mu</math>QFR (95% CI)</b>	<b>0.81 (0.76–0.85)</b>	<b>0.79 (0.73–0.85)</b>	<b>0.85 (0.77–0.94)</b>	<b>0.204</b>

Data presented as counts (percent), mean (standard deviation) or median (P<sub>25</sub> – P<sub>75</sub>); 3D-QFR — three-dimensional quantitative flow ratio; BMI — body mass index; CI — confidence interval; DS — diameter stenosis; GFR — glomerular filtration rate by Cockcroft-Gault method; LAD — left anterior descending artery; LCX — left circumflex artery; LVEF — left ventricular ejection fraction; MLD — minimal lumen diameter; MI — myocardial infarction; OAD — oral antidiabetics; PCI — percutaneous coronary intervention; RCA — right coronary artery; RVD — reference vessel diameter;  $\mu$ QFR (microQFR) — single angiographic view quantitative flow ratio

ably performed. In the current retrospective study, 12.24% of the arteries were unsuitable for standard 3D-QFR, in line with previous retrospective re-

ports, in which the unfeasibility was around 15% [19, 22]. This retrospective feasibility is sensibly lower than that reported for prospective stud-

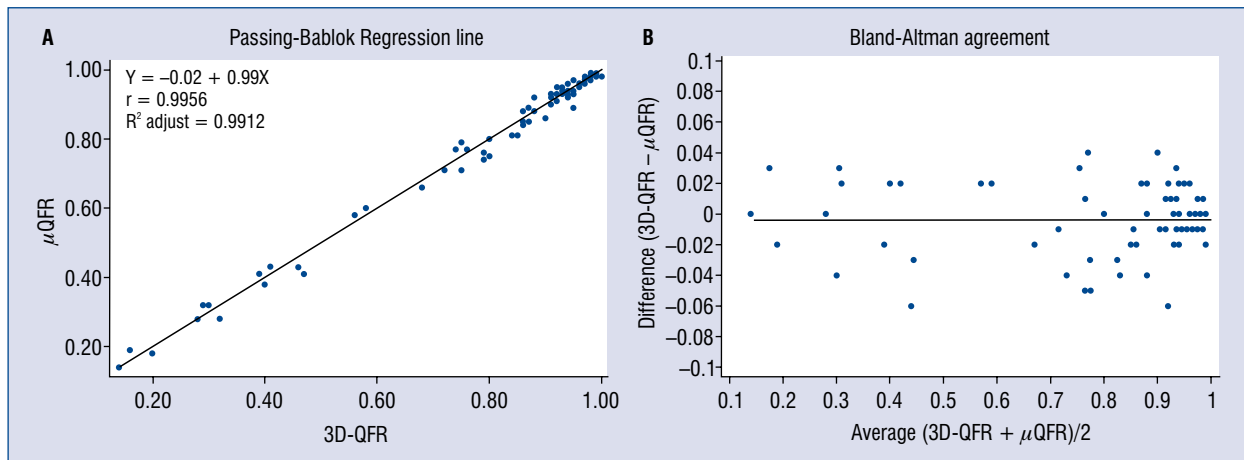


**Figure 3.** Agreement between three-dimensional quantitative flow ratio (3D-QFR) and single angiographic view quantitative flow ratio ( $\mu$ QFR) estimated by orthogonal regression line in panel **A** (Passing-Bablok method) and Bland-Altman graphics in panel **B**.

ies [15, 17], wherein a dedicated acquisition was upfront pursued to optimize the QFR calculation. This aspect might be important not only for scientific purposes, but also for clinical applications, for instance to avoid staged procedures in non-infarct-related artery lesions after primary percutaneous coronary intervention [26, 27].

Likewise, the excellent agreement of  $\mu$ QFR with standard 3D-QFR methods reassures the results reported in previous studies, in which the novel method proved excellent diagnostic accuracy, as compared with wire-based FFR [23]. This methodologically simplified but still accurate method could help to increase the penetration of physiology in routine clinical practice, which is still suboptimal in real-life [6–10]. Indeed, current evidence can hardly justify the use of plain angiography for decision-making about the need of revascularization in stable coronary heart disease, as physiology-guided revascularization has consistently proven superior clinical outcomes to anatomy-guided revascularization [1–5].

**Limitations of the study**

The retrospective design of the present study might be regarded as a limitation, as it controls the possibility of selection bias in an imperfect way, notwithstanding the careful methodological design. Nonetheless, the retrospective design was explicitly preferred in this case, because it was the setting in which eventual differences in feasibility was most likely to be unravelled.

The analysis was centrally performed offline by highly expert analysts in a certified corelab.

The agreement onsite between both methods, performed by local operators should be appraised in future studies.

The 3D-QFR used in this study (Pulse Medical, Shanghai, China) also takes into account the fractal geometry at the bifurcations. This might have favoured the optimal agreement between the methods, which might be not directly extrapolated to other methods of computational physiology which do not take Murray’s law into account.

The accuracy of  $\mu$ QFR could be theoretically jeopardized in highly eccentric lesions, in which the differences in computed QFR between angiographic projections might be exaggerated. In the study sample, this theoretical inaccuracy was not clearly unveiled in any single case. The retrospective design, relying exclusively on angiography, makes the assessment of eccentricity somewhat difficult and subjective in the current study, but it is worthy of specific clarification in future studies.

**Conclusions**

Murray-law based quantitative flow ratio using a single angiographic projection showed excellent agreement with standard 3D-QFR and improved the feasibility of the latter in retrospective studies. These results encourage the interchangeable use of  $\mu$ QFR whenever a proper 3D-QFR cannot be reliably calculated due to lack of suitable double projections.

**Conflict of interest:** None declared

## References

1. Bech GJ, De Bruyne B, Pijls NH, et al. Fractional flow reserve to determine the appropriateness of angioplasty in moderate coronary stenosis: a randomized trial. *Circulation*. 2001; 103(24): 2928–2934, doi: [10.1161/01.cir.103.24.2928](https://doi.org/10.1161/01.cir.103.24.2928), indexed in Pubmed: [11413082](https://pubmed.ncbi.nlm.nih.gov/11413082/).
2. Tonino PAL, De Bruyne B, Pijls NHJ, et al. Fractional flow reserve versus angiography for guiding percutaneous coronary intervention. *N Engl J Med*. 2009; 360(3): 213–224, doi: [10.1056/NEJMoa0807611](https://doi.org/10.1056/NEJMoa0807611), indexed in Pubmed: [19144937](https://pubmed.ncbi.nlm.nih.gov/19144937/).
3. De Bruyne B, Pijls NHJ, Kalesan B, et al. Fractional flow reserve-guided PCI versus medical therapy in stable coronary disease. *N Engl J Med*. 2012; 367(11): 991–1001, doi: [10.1056/NEJMoa1205361](https://doi.org/10.1056/NEJMoa1205361), indexed in Pubmed: [22924638](https://pubmed.ncbi.nlm.nih.gov/22924638/).
4. Davies J, Sen S, Dehbi HM, et al. Use of the Instantaneous Wave-free Ratio or Fractional Flow Reserve in PCI. *N Engl J Med*. 2017; 376(19): 1824–1834, doi: [10.1056/nejmoa1700445](https://doi.org/10.1056/nejmoa1700445).
5. Götberg M, Christiansen E, Gudmundsdottir I, et al. Instantaneous wave-free ratio versus fractional flow reserve to guide PCI. *N Engl J Med*. 2017; 376(19): 1813–1823, doi: [10.1056/nejmoa1616540](https://doi.org/10.1056/nejmoa1616540).
6. Toth G, Toth B, Johnson N, et al. Revascularization Decisions in Patients With Stable Angina and Intermediate Lesions. *Circ Cardiovasc Interv*. 2014; 7(6): 751–759, doi: [10.1161/circinterventions.114.001608](https://doi.org/10.1161/circinterventions.114.001608).
7. Härle T, Zeymer U, Hochadel M, et al. Real-world use of fractional flow reserve in Germany: results of the prospective ALKK coronary angiography and PCI registry. *Clin Res Cardiol*. 2017; 106(2): 140–150, doi: [10.1007/s00392-016-1034-5](https://doi.org/10.1007/s00392-016-1034-5), indexed in Pubmed: [27599974](https://pubmed.ncbi.nlm.nih.gov/27599974/).
8. Lee HS, Lee JM, Nam CW, et al. Consensus document for invasive coronary physiologic assessment in Asia-Pacific countries. *Cardiol J*. 2019; 26(3): 215–225, doi: [10.5603/CJ.a2019.0054](https://doi.org/10.5603/CJ.a2019.0054), indexed in Pubmed: [31225632](https://pubmed.ncbi.nlm.nih.gov/31225632/).
9. Gutiérrez-Chico JL, Zhao S, Chatzizisis YS. Vorticity: at the crossroads of coronary biomechanics and physiology. *Atherosclerosis*. 2018; 273: 115–116, doi: [10.1016/j.atherosclerosis.2018.04.001](https://doi.org/10.1016/j.atherosclerosis.2018.04.001), indexed in Pubmed: [29665968](https://pubmed.ncbi.nlm.nih.gov/29665968/).
10. Gutiérrez-Chico JL. Planning percutaneous interventions with optical flow ratio: “niu” odds in favour of imaging in the year of the Ox. *EuroIntervention*. 2021; 17(12): e958–e960, doi: [10.4244/EIJV1712A160](https://doi.org/10.4244/EIJV1712A160), indexed in Pubmed: [34916180](https://pubmed.ncbi.nlm.nih.gov/34916180/).
11. Ojeda S, Romaguera R, Cruz-González I, et al. [Spanish Cardiac Catheterization and Coronary Intervention Registry. 29th Official Report of the Interventional Cardiology Association of the Spanish Society of Cardiology (1990-2019)]. *Rev Esp Cardiol*. 2020; 73(11): 927–936, doi: [10.1016/j.recesp.2020.07.024](https://doi.org/10.1016/j.recesp.2020.07.024), indexed in Pubmed: [33012949](https://pubmed.ncbi.nlm.nih.gov/33012949/).
12. Neumann F-J, Sousa-Uva M, Ahlsson A, et al. 2018 ESC/EACTS Guidelines on myocardial revascularization. *Eur Heart J*. 2019; 40: 87–165, doi: [10.1093/eurheartj/ehy394](https://doi.org/10.1093/eurheartj/ehy394), indexed in Pubmed: [30165437](https://pubmed.ncbi.nlm.nih.gov/30165437/).
13. Tebaldi M, Biscaglia S, Fineschi M, et al. Evolving Routine Standards in Invasive Hemodynamic Assessment of Coronary Stenosis: The Nationwide Italian SICI-GISE Cross-Sectional ERIS Study. *JACC Cardiovasc Interv*. 2018; 11(15): 1482–1491, doi: [10.1016/j.jcin.2018.04.037](https://doi.org/10.1016/j.jcin.2018.04.037), indexed in Pubmed: [29803695](https://pubmed.ncbi.nlm.nih.gov/29803695/).
14. Gutiérrez-Chico JL, Chen Y, Yu W, et al. Diagnostic accuracy and reproducibility of optical flow ratio for functional evaluation of coronary stenosis in a prospective series. *Cardiol J*. 2020; 27(4): 350–361, doi: [10.5603/CJ.a2020.0071](https://doi.org/10.5603/CJ.a2020.0071), indexed in Pubmed: [32436590](https://pubmed.ncbi.nlm.nih.gov/32436590/).
15. Tu S, Barbato E, Kőszegi Z, et al. Fractional flow reserve calculation from 3-dimensional quantitative coronary angiography and TIMI frame count: a fast computer model to quantify the functional significance of moderately obstructed coronary arteries. *JACC Cardiovasc Interv*. 2014; 7(7): 768–777, doi: [10.1016/j.jcin.2014.03.004](https://doi.org/10.1016/j.jcin.2014.03.004), indexed in Pubmed: [25060020](https://pubmed.ncbi.nlm.nih.gov/25060020/).
16. Li Y, Gutiérrez-Chico JL, Holm NR, et al. Impact of side branch modeling on computation of endothelial shear stress in coronary artery disease: coronary tree reconstruction by fusion of 3D angiography and OCT. *J Am Coll Cardiol*. 2015; 66(2): 125–135, doi: [10.1016/j.jacc.2015.05.008](https://doi.org/10.1016/j.jacc.2015.05.008), indexed in Pubmed: [26160628](https://pubmed.ncbi.nlm.nih.gov/26160628/).
17. Tu S, Westra J, Yang J, et al. Diagnostic Accuracy of Fast Computational Approaches to Derive Fractional Flow Reserve From Diagnostic Coronary Angiography: The International Multicenter FAVOR Pilot Study. *JACC Cardiovasc Interv*. 2016; 9(19): 2024–2035, doi: [10.1016/j.jcin.2016.07.013](https://doi.org/10.1016/j.jcin.2016.07.013), indexed in Pubmed: [27712739](https://pubmed.ncbi.nlm.nih.gov/27712739/).
18. Collet C, Onuma Y, Sonck J, et al. Diagnostic performance of angiography-derived fractional flow reserve: a systematic review and Bayesian meta-analysis. *Eur Heart J*. 2018; 39(35): 3314–3321, doi: [10.1093/eurheartj/ehy445](https://doi.org/10.1093/eurheartj/ehy445), indexed in Pubmed: [30137305](https://pubmed.ncbi.nlm.nih.gov/30137305/).
19. Cortés C, Carrasco-Moraleja M, Aparisi A, et al. Quantitative flow ratio-meta-analysis and systematic review. *Catheter Cardiovasc Interv*. 2021; 97(5): 807–814, doi: [10.1002/ccd.28857](https://doi.org/10.1002/ccd.28857), indexed in Pubmed: [32196932](https://pubmed.ncbi.nlm.nih.gov/32196932/).
20. Yu W, Tanigaki T, Ding D, et al. Accuracy of intravascular ultrasound-based fractional flow reserve in identifying hemodynamic significance of coronary stenosis. *Circ Cardiovasc Interv*. 2021; 14(2): e009840, doi: [10.1161/CIRCINTERVENTIONS.120.009840](https://doi.org/10.1161/CIRCINTERVENTIONS.120.009840), indexed in Pubmed: [33541105](https://pubmed.ncbi.nlm.nih.gov/33541105/).
21. Li Z, Zhang J, Xu L, et al. Diagnostic accuracy of a fast computational approach to derive fractional flow reserve from coronary CT angiography. *JACC Cardiovasc Imaging*. 2020; 13(1 Pt 1): 172–175, doi: [10.1016/j.jcmg.2019.08.003](https://doi.org/10.1016/j.jcmg.2019.08.003), indexed in Pubmed: [31542542](https://pubmed.ncbi.nlm.nih.gov/31542542/).
22. Cortés C, Rivero F, Gutiérrez-Ibañes E, et al. Prospective validation and comparison of new indexes for the assessment of coronary stenosis: resting full-cycle and quantitative flow ratio. *Rev Esp Cardiol (Engl Ed)*. 2021; 74(1): 94–97, doi: [10.1016/j.rec.2020.05.039](https://doi.org/10.1016/j.rec.2020.05.039), indexed in Pubmed: [32792309](https://pubmed.ncbi.nlm.nih.gov/32792309/).
23. Tu S, Ding D, Chang Y, et al. Diagnostic accuracy of quantitative flow ratio for assessment of coronary stenosis significance from a single angiographic view: A novel method based on bifurcation fractal law. *Catheter Cardiovasc Interv*. 2021; 97 (Suppl 2): 1040–1047, doi: [10.1002/ccd.29592](https://doi.org/10.1002/ccd.29592), indexed in Pubmed: [33660921](https://pubmed.ncbi.nlm.nih.gov/33660921/).
24. Murray CD. The physiological principle of minimum work: I. The vascular system and the cost of blood volume. *Proc Natl Acad Sci U S A*. 1926; 12(3): 207–214, doi: [10.1073/pnas.12.3.207](https://doi.org/10.1073/pnas.12.3.207), indexed in Pubmed: [16576980](https://pubmed.ncbi.nlm.nih.gov/16576980/).
25. Zhao Q, Li C, Chu M, et al. Angiography-based coronary flow reserve: The feasibility of automatic computation by artificial intelligence. *Cardiol J*. 2021 [Epub ahead of print], doi: [10.5603/CJ.a2021.0087](https://doi.org/10.5603/CJ.a2021.0087), indexed in Pubmed: [34355775](https://pubmed.ncbi.nlm.nih.gov/34355775/).
26. Cortés C, Rodríguez-Gabella T, Gutiérrez H, et al. Quantitative flow ratio in myocardial infarction for the evaluation of non-infarct-related arteries. The QIMERA pilot study. *RECICE*. 2019, doi: [10.24875/recice.m19000007](https://doi.org/10.24875/recice.m19000007).
27. Zhang J, Yao M, Jia X, et al. The efficacy and safety of quantitative flow ratio-guided complete revascularization in patients with ST-segment elevation myocardial infarction and multivessel disease: A pilot randomized controlled trial. *Cardiol J*. 2021 [Epub ahead of print], doi: [10.5603/CJ.a2021.0111](https://doi.org/10.5603/CJ.a2021.0111), indexed in Pubmed: [34581424](https://pubmed.ncbi.nlm.nih.gov/34581424/).